

## Chapter 2

# Theoretical Framework and Motivation

The Standard Model is currently the most precise theoretical framework to describe the sub-atomic particles and their behavior, and a large number of precision measurements have validated its accuracy. However, there are still many problems that the SM leaves unsolved. This indicates that it is a low-energy approximation of a more general underlying theory, and new physics beyond the SM does exist. Supersymmetry, which is a symmetry that relates bosons and fermions, is one of the most promising theories providing a solution to the problems in the SM. This chapter gives an overview of the SUSY models explored in this dissertation and their theoretical motivations.

### 2.1 The Standard Model

The SM is a relativistic quantum field theory that incorporates the basic principles of quantum mechanics and special relativity. The SM incorporates successfully three out of four fundamental interactions in nature: the electromagnetic, the weak and the strong interactions. The SM Lagrangian describes a non-Abelian gauge symmetry that refers to the group  $SU(3)_C \otimes SU(2)_L \otimes U(1)_Y$ , where the  $SU(3)_C$  group refers to the quantum chromodynamics (QCD), the theory describing the interactions of quark and gluons by the color charge, while the  $SU(2)_L \otimes U(1)_Y$  group refers to the electroweak interactions. The interactions are mediated by gauge bosons: gluons (strong interactions), photons (electromagnetic interaction), and the W and Z bosons (weak interactions).

All matter in nature is made up of elementary particles, called fermions. Figure 2.1 summarizes the elementary particles that appear in the SM. Their internal quantum numbers are also shown in the figure. The fermions can be subdivided by the interactions in which they participate. Quarks take part in the strong, electromagnetic and weak interactions, while leptons do not take part in strong interactions. Leptons and

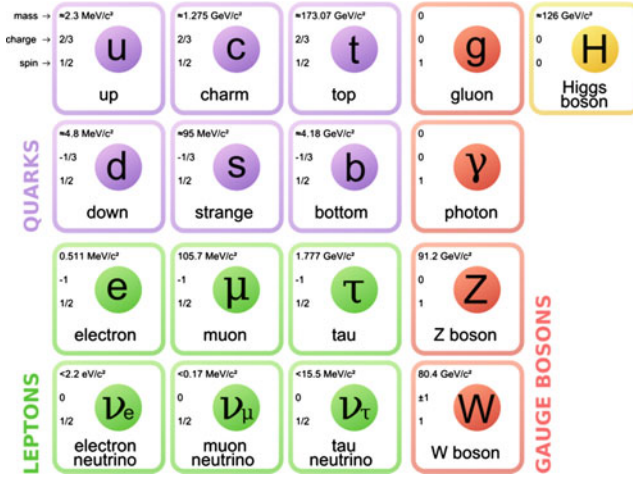


**Fig. 2.1** List of elementary particles in the standard model. Figure from [5]

quarks are arranged in three families, each family containing one charged lepton, one neutrino, and one up- and one down-type quark.

The masses of all elementary particles are given by the interaction with the Higgs field [1, 2]. The last piece of the SM, the Higgs boson, had been searched for at many research facilities around the world, but it was not discovered until 2012. In 2012, the ATLAS and CMS collaborations reported the strong evidence of a SM-like Higgs boson with a mass of  $\sim 126 \text{ GeV}$  [3, 4]. So far, the measured couplings of the boson to the SM particles are consistent with those of the SM Higgs boson.

### 2.1.1 Outstanding Issues in the Standard Model

The SM has succeeded in explaining the wide experimental results. In spite of its success, it cannot be the ultimate description of the universe. As previously mentioned, the SM only describes three out of four fundamental interactions in nature. The SM is therefore not a theory of everything. In addition to this, the SM raises three fundamental problems without providing the answers: the hierarchy problem, the grand unification and the existence of dark matter.

#### 2.1.1.1 Hierarchy Problem

One of the most problematic aspects of the SM is the numerical value of the Higgs boson mass. The Higgs boson receives large radiative corrections to its mass, which comes from loop diagrams. For example, given a Dirac fermion  $f$  that receives its

mass from the Higgs boson, the mass squared of the Higgs boson ( $m_h^2$ ) is given by

$$m_h^2 \approx m_{h, \text{bare}}^2 + m_{h, 1\text{-loop}}^2 \quad (2.1)$$

$$= m_{h, \text{bare}}^2 - \frac{\lambda_f^2}{8\pi^2} N_c^f \int^{\Lambda} \frac{d^4 p}{p^2} \quad (2.2)$$

$$\approx m_{h, \text{bare}}^2 + \frac{\lambda_f^2}{8\pi^2} N_c^f \Lambda^2, \quad (2.3)$$

where  $m_h$  is the physical Higgs boson mass that is measured to be  $\sim 126 \text{ GeV}$ ,  $m_{h, \text{bare}}$  is the bare Higgs boson mass,  $\lambda_f$  is the Yukawa coupling constant,  $N_c^f$  is the number of colors of fermion  $f$  and  $\Lambda$  is the largest energy scale where the standard model is valid. For large  $\Lambda$ , the bare mass and the 1-loop correction must cancel to give the physical Higgs boson mass. If  $\Lambda$  is close to the Planck scale  $\approx 10^{19} \text{ GeV}$ , Eq. 2.3 implies  $N^0 \equiv m_{h, \text{bare}}^2/m_h^2 \sim 10^{30}$ ; a fine-tuning of 1 part in  $10^{30}$ .

SUSY moderates this fine-tuning [6]. If SUSY is exact and an unbroken symmetry, the Higgs boson mass receives no perturbative corrections. Due to SUSY breaking, the Higgs boson mass becomes

$$m_h^2 \approx m_{h, \text{bare}}^2 + \frac{\lambda_{\tilde{f}}^2}{8\pi^2} N_c^{\tilde{f}} (m_{\tilde{f}}^2 - m_f^2) \ln (\Lambda^2/m_{\tilde{f}}^2), \quad (2.4)$$

where  $\tilde{f}$  is the superpartner of fermion  $f$ . The quadratic dependence on  $\Lambda$  is reduced to a logarithmic one, and the Higgs boson mass is natural if  $m_{\tilde{f}}$  is not too far above  $m_f$ . The upper bound on sfermion masses is given by

$$m_{\tilde{f}} \leq 800 \text{ GeV} \frac{1}{\lambda_f} \left( \frac{3}{N_c^f} \right)^{\frac{1}{2}} \left( \frac{70}{\ln(\Lambda^2/m_{\tilde{f}}^2)} \right)^{\frac{1}{2}} \left( \frac{N^0}{100} \right)^{\frac{1}{2}}, \quad (2.5)$$

where  $\lambda_f$  and  $N_c^f$  are normalized to values for top quark and the logarithm term ( $N^0$ ) is normalized to the value for  $\Lambda \sim 10^{19} \text{ GeV}$  (1 % fine-tuning), respectively.

### 2.1.1.2 Grand Unification

In the SM, the strong, weak, and electromagnetic gauge couplings do not unify at any scale. However, in the minimal supersymmetric standard model (MSSM) [7], which is described later, the gauge coupling renormalization group equations are modified above the superpartner mass scale. If the superpartners are roughly at the weak scale, the gauge couplings unify at  $\sim 10^{16} \text{ GeV}$  as shown in Fig. 2.2 [7]. This fact further motivates both the grand unification and weak-scale supersymmetry.

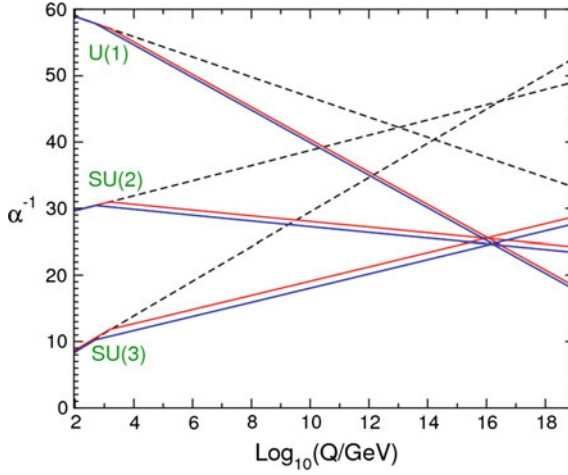


**Fig. 2.2** Predictions for the running of the inverse gauge couplings from the renormalization group equations. The evolution of coupling constants is shown by the *dashed lines* for the SM and by the *solid lines* for the MSSM. The difference between the *blue* and *red solid lines* originates from varying the supersymmetric particle masses between 500 GeV and 1.5 TeV and from varying  $\alpha(M_Z)$  between 0.117 and 0.121. Figure from [7]

### 2.1.1.3 Dark Matter

The bulk of observable matter in the universe is constituted by baryons and electrons. However, predictions on the total mass of baryonic matter in the universe from cosmic ray measurements are in contrast to those of gravitational effects. Therefore, the matter described by the SM makes up only approximately 5 % of the universe from cosmological observations, and a large part ( $\sim 22\%$ ) is considered to consist of neutral, only weakly interacting, dark matter. The SM gives no explanation for the amount of dark matter present in the universe. There are various hypotheses on dark matter depending on the mass and velocity of the particles: hot, warm, and cold dark matter. Since the velocity of warm, hot dark matter is quite high, they cannot explain the structure of the universe, and are not regarded as the main composition of dark matter. The most popular choice is cold dark matter. According to the latest measurements of the anisotropy of the cosmic microwave background and of the spatial distribution of galaxies [8], the density of cold, non-baryonic matter is calculated to be  $\Omega_{\text{nbm}} h^2 = 0.112 \pm 0.006$ , where  $h$  is the Hubble constant in units of 100 km/(s·Mpc). SUSY provides an excellent dark matter candidate when the neutralino is the LSP.

### 2.1.1.4 Gravity

The SM does not include any description of gravity. Any attempts to incorporate the theory of general relativity into the SM have not been successful so far. While

gravitational effects at the electroweak scale are negligible, they become significant at the Planck scale and are of equal strength as the other forces. Since two successive supersymmetric transformations give rise to a translation in space-time, gravity would automatically be a part of supersymmetric models.

## 2.2 Supersymmetry

As described in the previous section, the SM is not a complete theory, and new physics beyond the SM exists. Supersymmetry is one of the most promising theories providing a solution to the problems in the SM. It establishes a symmetry between fermions and bosons. The SUSY must be a broken symmetry since no supersymmetric particles with the same mass as their SM partners have been observed. Therefore, the masses of the superpartners must be heavier than those of their SM partners.

### 2.2.1 Minimal Supersymmetric Standard Model

The MSSM is the simplest supersymmetric extension of the SM. Its particle content is summarized in Table 2.1

As the left- and right-handed states transform differently under the gauge group, individual particles are introduced for left- and right-handed fermions. These left- and right-handed supersymmetric states refer to not their own helicity but that of their SM partner. The superpartners of fermions are called squarks and sleptons while the superpartners of gauge bosons are called gluino, wino, and photino. The gravitino is the only particle having a spin of  $3/2$ . The gauge interactions and couplings of the particles are the same as those of their SM partners.

In the SM, the electroweak symmetry is broken by introducing the Higgs mechanism, and one Higgs doublet gives masses to all particles. In the MSSM, the electroweak gauge symmetry suffers from a gauge anomaly, therefore, a Higgs field must be a weak isodoublet. One of the two Higgs supermultiplets has the Yukawa coupling that gives masses to the up-type quarks with the hypercharge  $Y = 1/2$ , and the Yukawa coupling of the other doublet ( $Y = -1/2$ ) gives masses to the down-type quarks and the charged leptons. They are denoted by  $H_u$  and  $H_d$ , respectively, and the vacuum expectation values (VEVs) of  $H_u^0$  and  $H_d^0$  are written as

$$v_u = \langle H_u^0 \rangle, \quad v_d = \langle H_d^0 \rangle. \quad (2.6)$$

These VEVs are related to the SM parameters by

$$v_u^2 + v_d^2 = v^2 = \frac{2m_Z^2}{g_1^2 + g_2^2}, \quad (2.7)$$

**Table 2.1** Supersymmetric particles in the MSSM

Name	Spin	Gauge eigenstates	Mass eigenstates
Squarks	0	$\tilde{u}_L, \tilde{u}_R, \tilde{d}_L, \tilde{d}_R$	
		$\tilde{c}_L, \tilde{c}_R, \tilde{s}_L, \tilde{s}_R$	
		$\tilde{t}_L, \tilde{t}_R, \tilde{b}_L, \tilde{b}_R$	$\tilde{t}_1, \tilde{t}_2, \tilde{b}_1, \tilde{b}_2$
Sleptons	0	$\tilde{e}_L, \tilde{e}_R, \tilde{\nu}_e$	
		$\tilde{\mu}_L, \tilde{\mu}_R, \tilde{\nu}_\mu$	
		$\tilde{\tau}_L, \tilde{\tau}_R, \tilde{\nu}_\tau$	$\tilde{\tau}_1, \tilde{\tau}_2, \tilde{\nu}_\tau$
Higgs bosons	0	$H_u^0, H_d^0, H_u^+, H_d^-$	$h^0, H^0, A^0, H^\pm$
Neutralinos	1/2	$\tilde{B}^0, \tilde{W}^0, \tilde{H}_u^0, \tilde{H}_d^0$	$\tilde{\chi}_1^0, \tilde{\chi}_2^0, \tilde{\chi}_3^0, \tilde{\chi}_4^0$
Charginos	1/2	$\tilde{W}^\pm, \tilde{H}_u^\pm, \tilde{H}_d^\pm$	$\tilde{\chi}_1^\pm, \tilde{\chi}_2^\pm$
Gluino	1/2	$\tilde{g}$	
Gravitino	3/2	$\tilde{G}$	

where  $v$ ,  $g_1$  and  $g_2$  are VEVs of the SM Higgs boson, the gauge coupling constants of  $U(1)_Y$  and  $SU(2)_L$  gauge groups, respectively. The ratio of the VEVs is an important parameter and set to be free in the theory, and it is traditionally written as

$$\tan \beta \equiv \frac{v_u}{v_d}. \quad (2.8)$$

These two doublets have eight degrees of freedom. Three are absorbed by the gauge bosons of the weak interaction as in the SM, leaving five physical Higgs bosons. These five Higgs scalar mass eigenstates consist of two CP-even neutral scalars  $h^0$  and  $H^0$ , one CP-odd neutral scalar  $A^0$ , and charged scalars  $H^\pm$ .

The superpartners of the Higgs bosons are called Higgsinos, denoted by  $\tilde{H}_u$  and  $\tilde{H}_d$  for the  $SU(2)_L$ -doublet left-handed spinor fields, with weak isospin components  $(\tilde{H}_u^+, \tilde{H}_u^0)$  and  $(\tilde{H}_d^0, \tilde{H}_d^-)$ . The mass of Higgsinos is given by  $\mu_H$ .

The superpartners of the SM gauge bosons, arranged in gauge supermultiplets, are not the mass eigenstates of the MSSM. The Higgsinos and electroweak gauginos mix with each other due to the effects of the electroweak symmetry breaking. The neutral Higgsinos ( $\tilde{H}_u^0$  and  $\tilde{H}_d^0$ ) and the neutral gauginos ( $\tilde{B}^0$  and  $\tilde{W}^0$ ) combine to form four mass eigenstates called neutralinos  $\tilde{\chi}_i^0 (i = 1, 2, 3, 4)$ . The charged Higgsinos ( $\tilde{H}_u^+$  and  $\tilde{H}_d^-$ ) and winos ( $\tilde{W}^+$  and  $\tilde{W}^-$ ) mix to form two mass eigenstates with charge  $\pm 1$  called charginos  $\tilde{\chi}_i^\pm (i = 1, 2)$ . The neutralinos are Majorana fermions in the MSSM.

### 2.2.2 *R*-parity

In the SM, the baryon number and lepton number are conserved since no possible renormalizable Lagrangian terms can introduce the violation of such numbers. In the MSSM, the most general gauge-invariant renormalizable superpotential contains the

terms that violate the conservation of the baryon number and lepton number, inducing the rapid proton decay. Since this decay has not been confirmed experimentally, these terms need to be suppressed. Therefore, an additional quantum number called  $R$ -parity, is defined as

$$R = (-1)^{2S+3(B-L)}, \quad (2.9)$$

where  $S$ ,  $B$  and  $L$  is the spin, the baryon number, and the lepton number, respectively. Employing this definition results in  $R = 1$  ( $R = -1$ ) for all SM particles (SUSY particles). Assuming exact  $R$ -parity conservation indicates several significant consequences:

- SUSY particles can only be produced in pairs, resulting in two decay chains.
- Eventually, every sparticle decays into the LSP.
- The LSP is stable. It behaves like neutrinos and escapes from detection, resulting in a noticeable amount of missing transverse momentum (and its magnitude  $E_T^{\text{miss}}$ ) in collider experiments. If the LSP is neutral and has no color, it can be considered as a viable dark matter candidate.

The phenomenology of  $R$ -parity violating models is quite different because the LSP decays into SM particles. Throughout this dissertation,  $R$ -parity is assumed to be conserved.

### 2.2.3 SUSY Breaking Model

Since it is difficult to construct a realistic model of spontaneous SUSY breaking from the interaction between the particles in the MSSM, a hidden sector is introduced, which consists of particles that are completely neutral with respect to the SM gauge group. The SUSY breaking is assumed to occur in the hidden sector, and its effects are mediated to the visible sector by some mechanisms. In the general MSSM, 105 free parameters are added to the 19 of the SM. Assuming a specific breaking mechanism reduces the number of free parameters that determine the masses of all SUSY particles and their mixing.

## 2.3 Wino LSP Scenarios and Their Phenomenology

In this analysis, one of the most prominent models called Anomaly-Mediated Supersymmetry Breaking is explored.

### 2.3.1 Anomaly-Mediated Supersymmetry Breaking Model

Anomaly-Mediated Supersymmetry Breaking Model has no direct tree level coupling that mediates the SUSY breaking in the hidden sector to the observable sector. A

conformal anomaly in the auxiliary field of the supergravity multiplet mediates the SUSY breaking to the observable sector, and the AMSB model does not require any singlet SUSY breaking fields (i.e. the Polonyi fields), and hence, are free from the cosmological Polonyi problem [9, 10].

In the AMSB model, the masses of gauginos are generated at one-loop, while those of the scalar bosons are generated at two-loop level, because of the conformal anomaly that breaks scale invariance. The bino, wino, and gluino masses ( $M_1$ ,  $M_2$  and  $M_3$ ) have a special property that they are proportional to the coefficients of the renormalization group equations for their corresponding gauge groups:

$$M_1 = \frac{g_1^2}{16\pi^2} \left( \frac{33}{5} m_{3/2} \right), \quad (2.10)$$

$$M_2 = \frac{g_2^2}{16\pi^2} (m_{3/2}), \quad (2.11)$$

$$M_3 = \frac{g_3^2}{16\pi^2} (-3m_{3/2}), \quad (2.12)$$

where  $g_3$  and  $m_{3/2}$  are the gauge coupling constants of  $SU(3)_C$  gauge groups and the gravitino mass, respectively. The mass relation between the gauginos becomes  $M_1 : M_2 : M_3 \approx 3 : 1 : 8$ . The masses of squarks and sleptons [11] are obtained as

$$M_{\tilde{u}_L}^2 = m_0^2 + \left( \frac{1}{2} - \frac{2}{3} \sin^2 \theta_W \right) M_Z^2 \cos 2\beta + \left( -\frac{11}{50} g_1^4 - \frac{3}{2} g_2^4 + 8g_3^4 \right) \frac{m_{3/2}^2}{(16\pi^2)^2}, \quad (2.13)$$

$$M_{\tilde{d}_L}^2 = m_0^2 + \left( -\frac{1}{2} + \frac{1}{3} \sin^2 \theta_W \right) M_Z^2 \cos 2\beta + \left( -\frac{11}{50} g_1^4 - \frac{3}{2} g_2^4 + 8g_3^4 \right) \frac{m_{3/2}^2}{(16\pi^2)^2}, \quad (2.14)$$

$$M_{\tilde{u}_R}^2 = m_0^2 + \frac{2}{3} \sin^2 \theta_W M_Z^2 \cos 2\beta + \left( -\frac{88}{25} g_1^4 + 8g_3^4 \right) \frac{m_{3/2}^2}{(16\pi^2)^2}, \quad (2.15)$$

$$M_{\tilde{d}_R}^2 = m_0^2 - \frac{1}{3} \sin^2 \theta_W M_Z^2 \cos 2\beta + \left( -\frac{22}{25} g_1^4 + 8g_3^4 \right) \frac{m_{3/2}^2}{(16\pi^2)^2}, \quad (2.16)$$

$$M_{\tilde{e}_L}^2 = m_0^2 + \left( -\frac{1}{2} + \sin^2 \theta_W \right) M_Z^2 \cos 2\beta + \left( -\frac{99}{50} g_1^4 - \frac{3}{2} g_2^4 \right) \frac{m_{3/2}^2}{(16\pi^2)^2}, \quad (2.17)$$

$$M_{\tilde{\nu}_e}^2 = m_0^2 + \frac{1}{2} M_Z^2 \cos 2\beta + \left( -\frac{99}{50} g_1^4 - \frac{3}{2} g_2^4 \right) \frac{m_{3/2}^2}{(16\pi^2)^2}, \quad (2.18)$$

$$M_{\tilde{e}_R}^2 = m_0^2 - \sin^2 \theta_W M_Z^2 \cos 2\beta + \left( -\frac{198}{25} g_1^4 \right) \frac{m_{3/2}^2}{(16\pi^2)^2}, \quad (2.19)$$

where  $m_0$  and  $\theta_W$  are the universal scalar mass at the grand unification scale and the Weinberg angle, respectively.

In the AMSB model,  $m_0$  must be large otherwise the scalar leptons become tachyons. Then all sfermions become too heavy to be produced in hadron collider experiments. Figure 2.3 shows a sparticle mass spectrum for a certain parameter set of the AMSB model.



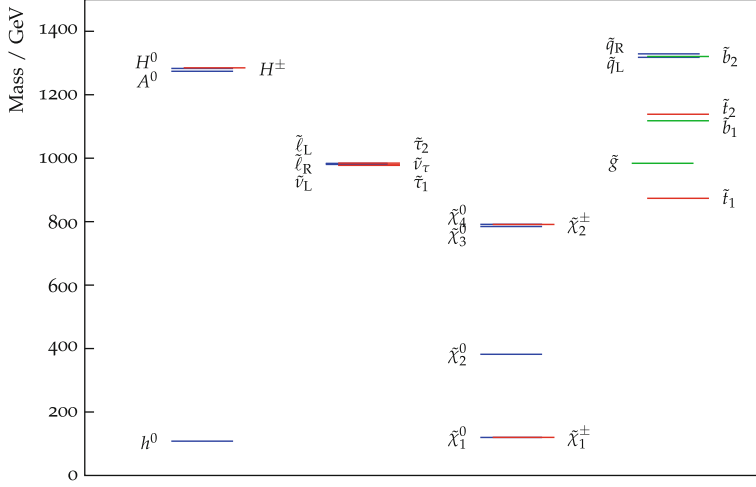


**Fig. 2.3** Sparticle mass spectrum for  $m_{3/2} = 32$  TeV,  $m_0 = 1000$  GeV,  $\tan \beta = 5$  and  $\mu_H > 0$

### 2.3.2 Pure Gravity Mediation Model

There is another well-motivated SUSY model that predicts the sparticle mass spectrum similar to that in the AMSB model, called Pure Gravity Mediation (PGM) model [12]. In this model, the gauginos obtain their masses by one-loop contributions in supergravity as in the AMSB model. The difference between the AMSB and PGM models is that the gauginos in the PGM model obtain their masses from additional contributions from threshold effects of the heavy Higgsinos. The gaugino masses are given by

$$M_1 = \frac{g_1^2}{16\pi^2} \frac{33}{5} \left( m_{3/2} + \frac{1}{11} L \right), \quad (2.20)$$

$$M_2 = \frac{g_2^2}{16\pi^2} (m_{3/2} + L), \quad (2.21)$$

$$M_3 = \frac{g_3^2}{16\pi^2} (-3m_{3/2}), \quad (2.22)$$

where  $L$  denotes the Higgsino threshold contribution given by

$$L \equiv \mu_H \sin 2\beta \frac{m_A^2}{|\mu_H|^2 - m_A^2} \ln \frac{|\mu_H|^2}{m_A^2}. \quad (2.23)$$

The size of the  $L$  parameter is expected to be of the order of the gravitino mass. In the limit for the  $L$  parameter to zero, the gaugino masses become the same ones in the AMSB model. The gluino mass is about eight times higher than the wino mass

for  $L = 0$  as in the AMSB model, while the gluino-to-wino mass ratio gets smaller for positive values of  $L$ .

### 2.3.3 Phenomenology

One prominent feature of these models is that the LSP is the pure neutral wino that is mass-degenerate with the charged wino. The lightest chargino  $\tilde{\chi}_1^\pm$  is slightly heavier than the lightest neutralino  $\tilde{\chi}_1^0$  due to radiative corrections involving electroweak gauge bosons. The typical mass splitting between  $\tilde{\chi}_1^\pm$  and  $\tilde{\chi}_1^0$  is  $\sim 160$  MeV as shown in Fig. 2.4, which implies that  $\tilde{\chi}_1^\pm$  has a considerable lifetime and predominantly decays into  $\tilde{\chi}_1^0$  plus a low-momentum ( $\sim 100$  MeV)  $\pi^\pm$ . Figure 2.5 shows  $\tau_{\tilde{\chi}_1^\pm}$  as a function of  $\Delta m_{\tilde{\chi}_1}$  on the assumption that  $\tilde{\chi}_1^\pm$  decays into  $\tilde{\chi}_1^0 + \pi^\pm$ . The decay width for this process is given as

$$\Gamma(\tilde{\chi}_1^\pm \rightarrow \tilde{\chi}_1^0 \pi^\pm) = \frac{2G_F^2}{\pi} \cos^2 \theta_c f_\pi^2 \Delta m_{\tilde{\chi}_1}^3 \left(1 - \frac{m_\pi^2}{\Delta m_{\tilde{\chi}_1}^2}\right)^{\frac{1}{2}}, \quad (2.24)$$

where  $G_F$ ,  $\theta_c$ ,  $f_\pi$  and  $m_\pi$  are the Fermi coupling constant, the Cabbibo angle, the pion decay constant ( $\simeq 130$  MeV), and the pion mass, respectively, resulting in a considerably long lifetime of the chargino:

**Fig. 2.4** Wino mass splitting  $\Delta m_{\tilde{\chi}_1}$  as a function of the chargino mass ( $m_{\tilde{\chi}_1^\pm}$ ) [13]. The dark green band shows  $\Delta m_{\tilde{\chi}_1}$  at the one-loop level with the uncertainty induced by the renormalization scale dependence and the red band shows  $\Delta m_{\tilde{\chi}_1}$  at two-loop

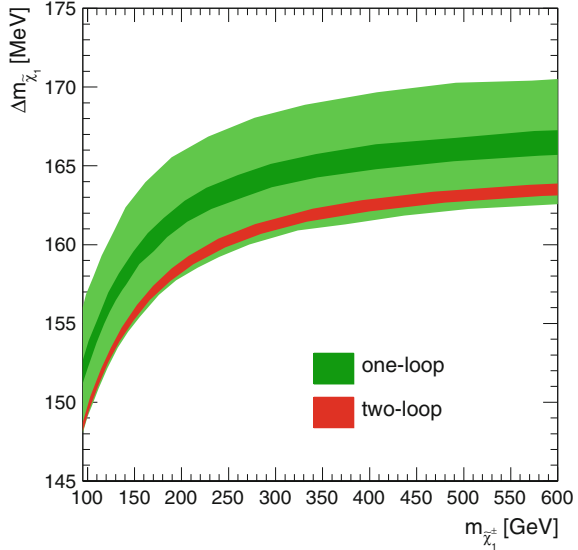
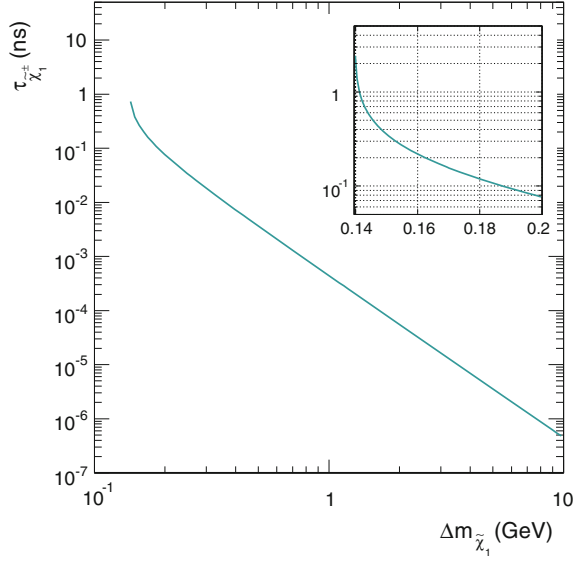


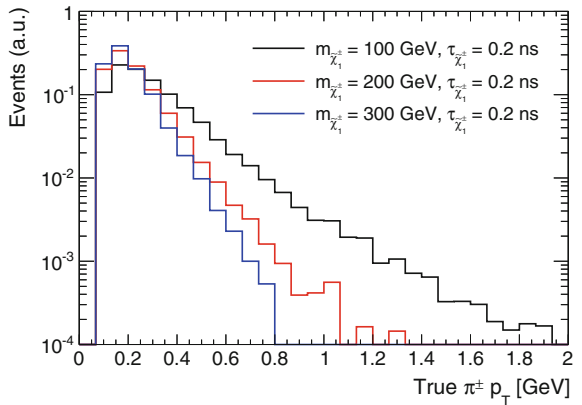
**Fig. 2.5** The  $\tau_{\tilde{\chi}_1^\pm}$  as a function of  $\Delta m_{\tilde{\chi}_1}$



$$c\tau_{\tilde{\chi}_1^\pm} \sim \mathcal{O}(\text{cm}) \quad (\tau_{\tilde{\chi}_1^\pm} \sim 0.2 \text{ ns}). \quad (2.25)$$

Therefore, a fraction of decaying charginos could be reconstructed as tracks in the collider experiments. The  $\tilde{\chi}_1^0$  escapes from detection and the softly emitted  $\pi^\pm$  is not reconstructed due to its low momentum as shown in Fig. 2.6. A track arising from a  $\tilde{\chi}_1^\pm$  with these characteristics is classified as a *disappearing track* that has few associated hits in the outer part of the tracking volume.

**Fig. 2.6** The  $p_T$  spectrum of  $\pi^\pm$  in the chargino decays



### 2.3.4 Theoretical and Experimental Indications

There are several theoretical and experimental indications that motivate exploring wino LSP scenarios.

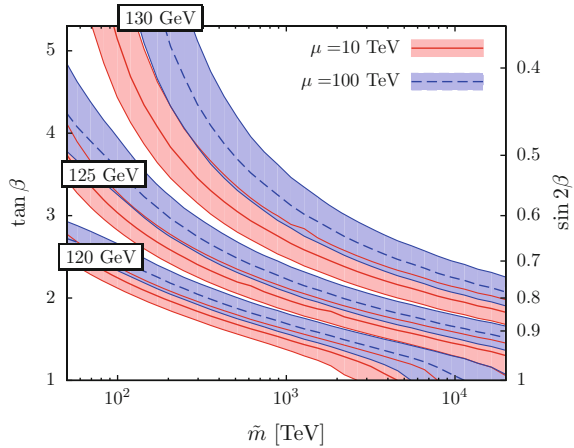
#### 2.3.4.1 Higgs Mass

The mass of the lightest Higgs boson ( $h^0$ ) in the MSSM is obtained by

$$m_{h^0}^2 \leq m_Z^2 \cos^2 2\beta + \frac{3}{4\pi^2} y_t^2 m_t^2 \sin^2 \beta \left( \log \frac{m_t^2}{m_{\tilde{t}}^2} + \frac{A_t^2}{m_{\tilde{t}}^2} - \frac{A_t^4}{12m_{\tilde{t}}^4} \right). \quad (2.26)$$

The Higgs mass is required to be less than the Z boson mass at tree level. While loop corrections increase this upper bound, the logarithmic term implies that the stop mass should be at least  $\mathcal{O}(10\text{--}100)\text{TeV}$  to realize the Higgs boson mass  $\sim 126\text{GeV}$  [3, 4]. Figure 2.7 shows a contour plot of the Higgs boson mass as a function of  $\tilde{m}$  and  $\tan\beta$ , where  $\tilde{m}$  is a typical sfermion mass [14]. This figure also indicates that the Higgs boson mass of  $\sim 126\text{GeV}$  is realized if  $\tilde{m}$  is  $\sim \mathcal{O}(10\text{--}100)\text{TeV}$  and the  $\tan\beta$  is  $\sim \mathcal{O}(1)$ . These features are consistent with the fact that any sfermions have not yet been observed at the LHC. The masses of sferimons in the AMSB model are generally large as stated before, therefore, the observed Higgs boson mass can be easily explained in the AMSB model.

**Fig. 2.7** Values of the Higgs boson mass in the  $\tilde{m}$ - $\tan\beta$  plane, where  $\tilde{m}$  is sfermion mass. The *solid (red)* curves represent ones with  $\mu_H = 10\text{TeV}$ , while the *dashed (blue)* curves  $\mu_H = 100\text{TeV}$ . The *shaded region* around each curve shows uncertainty from the top quark mass. Figure from [14]



### 2.3.4.2 Flavor Changing Neutral Current

The SUSY breaking terms for squark and slepton masses can induce too large FCNCs [15] since squark and slepton mass matrices can be new sources of flavor mixings and CP violation that are not related to the Cabibbo–Kobayashi–Maskawa matrix. With generic mass matrices and  $\mathcal{O}(1)$  CP violating phases,  $K^0 - \bar{K}^0$  mixing requires the squark masses to be greater than 1000 TeV. However, the problems of FCNCs and CP violation is not serious in the AMSB model since the soft SUSY breaking parameters are given by flavor-blind radiative corrections and the masses of squarks and sleptons are large.

### 2.3.4.3 Wino Dark Matter Scenario

The neutral wino can be the most natural candidate for dark matter. The thermal relic density of neutral wino can be the present mass density of dark matter if its mass is about 3.0 TeV [16]. For light winos with masses about a few hundred GeV, the measured relic abundance requires a non-thermal history with a late-decaying modulus [17] due to their large tree-level annihilation rate to W bosons. It has been argued that moduli with a mass of  $\mathcal{O}(100)$  TeV are consistent with Big Bang nucleosynthesis (BBN) and lead to the right relic abundance for light winos with masses about a few hundred GeV.

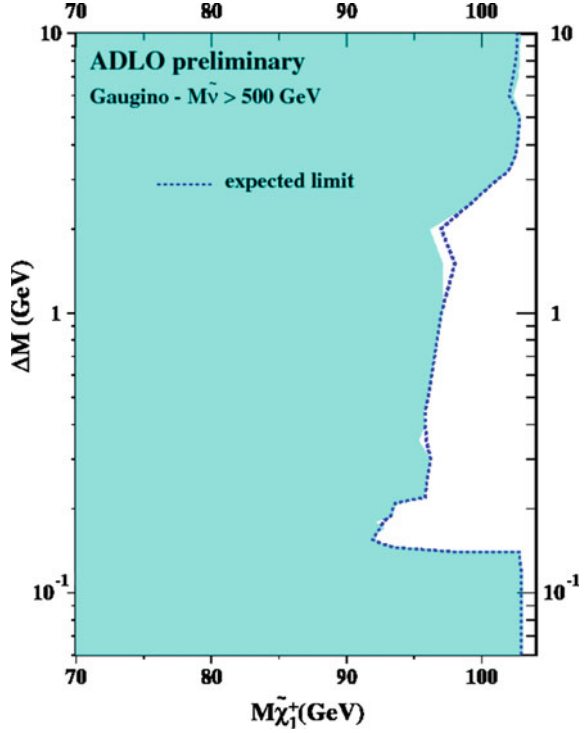
## 2.3.5 Previous Searches and Constraints

There are several constraints on wino LSP scenarios from collider experiments and indirect dark matter searches. Collider experiments can explore wino LSP scenarios and provide results that are largely independent of the model parameters. Indirect dark matter searches can provide complementary results and set limits on the wino dark matter especially in the non-thermal scenario, although they have a large uncertainty due to ambiguities of the dark matter profile, magnetic fields, and interstellar radiation density.

### 2.3.5.1 LEP2 Experiment

Searches for the charginos nearly mass-degenerate with the lightest neutralino were performed by experiments at LEP2 [18–20]. These analyzes are based on the events with a photon from ISR and the missing energy due to LSPs escaping the detector. Figure 2.8 shows the constraint on the  $\Delta m_{\tilde{\chi}_1 - m_{\tilde{\chi}_1^\pm}}$  space of the AMSB model by combining the LEP2 results, excluding the chargino having a mass up to 92 GeV [21].

**Fig. 2.8** Constraint on the  $\Delta m_{\tilde{\chi}_1^\pm - m_{\tilde{\chi}_1^\pm}}$  space derived by the results of the LEP2 experiments. Figure from [21]



### 2.3.5.2 ATLAS Experiment

Prior to the search described in this dissertation, a search for charginos nearly mass-degenerate with the lightest neutralino was also performed in  $pp$  collisions at  $\sqrt{s} = 7 \text{ TeV}$  with the ATLAS detector [22]. The analysis is dedicated to the direct chargino production process and is based on the disappearing track signature. Figures 2.9 and 2.10 show the constraint on the  $\tau_{\tilde{\chi}_1^\pm} - m_{\tilde{\chi}_1^\pm}$  space and  $\Delta m_{\tilde{\chi}_1^\pm - m_{\tilde{\chi}_1^\pm}}$  of the AMSB model, respectively. The previous result excludes the chargino having a mass up to  $130 \text{ GeV}$ .

### 2.3.5.3 Indirect Dark Matter Searches

There are a number of constraints on wino dark matter [23, 24] from indirect detection experiments of Fermi Gamma-Ray Space Telescope (Fermi) experiment [25] and High Energy Spectroscopic System (H.E.S.S.) experiment [26].

The Fermi result is derived by 24 months of data for ten satellite galaxies, and sets the limits on the annihilation cross-section of the wino dark matter by a search for the continuum photons generated mostly from the fragmentation of hadronic final states

**Fig. 2.9** Constraint on the  $\tau_{\tilde{\chi}_1^\pm} - m_{\tilde{\chi}_1^\pm}$  space in  $pp$  collisions at  $\sqrt{s} = 7$  TeV with the ATLAS detector [22]

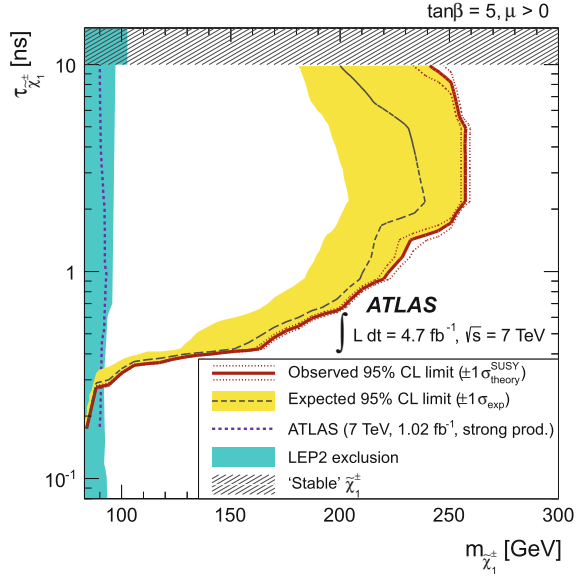
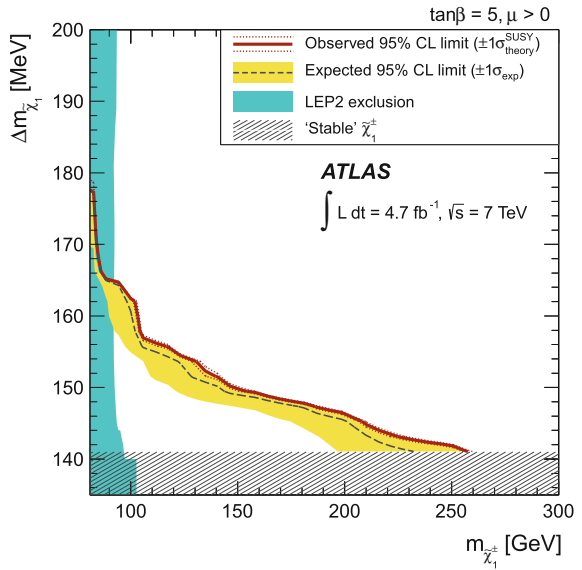


**Fig. 2.10** Constraint on the  $\Delta m_{\tilde{\chi}_1} - m_{\tilde{\chi}_1^\pm}$  space in  $pp$  collisions at  $\sqrt{s} = 7$  TeV with the ATLAS detector [22]



in the tree-level processes  $\tilde{\chi}_1^0 \tilde{\chi}_1^0 \rightarrow W^+ W^-$ . This is roughly comparable to that obtained from the antiproton flux measurement by PAMELA [27]. The antiproton measurement is subject to uncertainties related to their propagation models and dark matter profiles, therefore, PAMELA result is not shown in this dissertation.

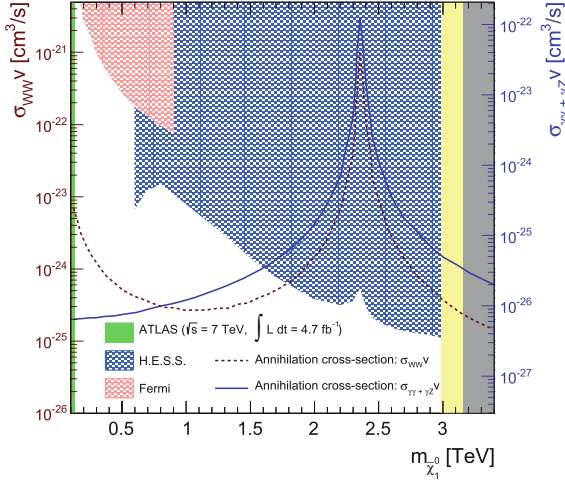


**Fig. 2.11** Constraints on the annihilation cross-section as a function of the wino mass [23]. The theoretical cross-section of annihilation into  $W^+ W^-$ ,  $\gamma \gamma$  and  $\gamma Z$  final states are also indicated by the *dashed red line* and the *solid blue line*, respectively. The excluded regions by the Fermi and H.E.S.S. experiments are indicated by the *shaded red region* and the *shaded blue region*, respectively. These exclusion contours are obtained on the assumption that the wino abundance is set by thermal freeze-out. The *shaded yellow region* between the *dotted lines* corresponds to  $\Omega h^2 = 0.12 \pm 0.06$ . In the *black shaded region*, a thermal wino exceeds the observed relic density

The H.E.S.S. collaboration investigated gamma-ray lines expected to arise from the one-loop processes  $\tilde{\chi}_1^0 \tilde{\chi}_1^0 \rightarrow \gamma \gamma$  and  $\tilde{\chi}_1^0 \tilde{\chi}_1^0 \rightarrow Z \gamma$  in a  $1^\circ$  radius circle at the Galactic Center, in which the Galactic plane is excluded by restricting the Galactic latitude to  $|b| > 0.3^\circ$ .

Figures 2.11 and 2.12 show the theoretical calculations of annihilation cross-section into  $W^+ W^-$ ,  $\gamma \gamma$  and  $\gamma Z$  final states and the constraints on the wino annihilation cross-section as a function of wino mass [23]. The wino relic density is assumed to equal to its thermal abundance in Fig. 2.11, while it is assumed to equal to the measured value due to a non-thermal history with a late-decaying modulus in Fig. 2.12. In the thermal scenario, the data from H.E.S.S. rules out wino dark matter in the mass range 1.6–3.1 TeV. In the non-thermal scenario, the data from Fermi and H.E.S.S. exclude wino dark matter in the ranges 100–500 GeV and 500 GeV–3.0 TeV, respectively. Note that the Fermi limit is approximately independent of uncertainties on dark matter profiles since the relevant unknown astrophysical parameters have already been marginalized over, while the H.E.S.S. limit assumes an NFW profile [28].

### 2.3.5.4 Direct Dark Matter Searches

The direct detection of dark matter can occur through their interaction with nuclei inside a detector. However, couplings of neutral wino to a Higgs boson or a Z boson



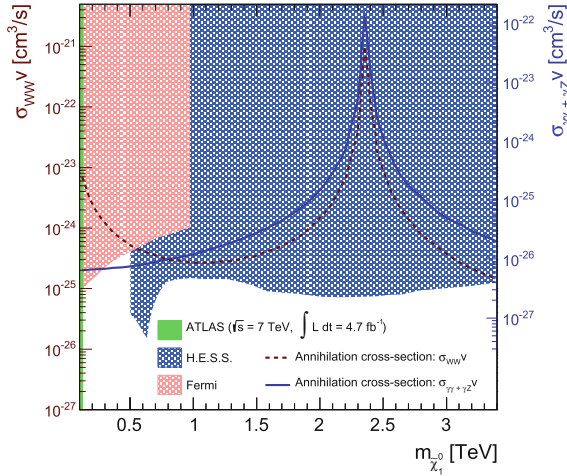


**Fig. 2.12** Constraints on the annihilation cross-section as a function of the wino mass [23]. The theoretical cross-section of annihilation into  $W^+ W^-$ ,  $\gamma \gamma$  and  $\gamma Z$  final states are also indicated by the *dashed red line* and the *solid blue line*, respectively. The excluded regions by the Fermi and H.E.S.S. experiments are indicated by the *shaded red region* and the *shaded blue region*, respectively. These exclusion contours are obtained on the assumption that the wino comprises all dark matter due to a non-thermal history

are highly suppressed at the tree-level, therefore, there has been no direct detection limits on wino LSP scenarios. The elastic scattering of a wino off a nucleon occurs at one-loop where wino couples to quarks and two-loop where wino couples to gluons in the nucleon. The associated spin-independent cross-section is  $\mathcal{O}(10^{-47}) \text{ cm}^2$  for winos [29, 30] having masses 50 GeV–3 TeV, which is well below the strongest direct detection limits from the Xenon100 experiment [31] and LUX experiment [32].

## References

1. F. Englert, R. Brout, Phys. Rev. Lett. **13**, 321 (1964)
2. P.W. Higgs, Phys. Lett. **12**, 132 (1964)
3. ATLAS Collaboration, Phys. Lett. **B716**, 1 (2012)
4. C.M.S. Collaboration, Phys. Lett. **B716**, 30 (2012)
5. [http://en.wikipedia.org/wiki/Standard\\_Model](http://en.wikipedia.org/wiki/Standard_Model)
6. J.L. Feng, Naturalness and the status of supersymmetry (2013). [arxiv:1302.6587](https://arxiv.org/abs/1302.6587) [hep-ph]
7. S.P. Martin, A supersymmetry primer (1997). [arXiv:hep-ph/9709356](https://arxiv.org/abs/hep-ph/9709356)
8. K. Nakamura et al., Particle data group. J. Phys. G **37**, 075021 (2010)
9. G.D. Coughlan et al., Phys. Lett. **B131**, 59 (1983)
10. M. Ibe, Y. Shinbara, T.T. Yanagida, Phys. Lett. **B639**, 534 (2006)
11. K. Huitu, J. Laamanen, P.N. Pandita, Phys. Rev. **D65**, 115003 (2010)
12. M. Ibe, S. Matsumoto, T.T. Yanagida, Phys. Rev. **D85**, 095011 (2012)
13. M. Ibe, S. Matsumoto, R. Sato, Phys. Lett. **B721**, 252 (2013)
14. L.J. Hall, Y. Nomura, S. Shirai, JHEP **1301**, 036 (2013)

15. F. Gabbiani, E. Gabrielli, A. Masiero, L. Silvestrini, Nucl. Phys. **B477**, 321 (1996)
16. J. Hisano, S. Matsumoto, M. Nagai, O. Saito, M. Senami, Phys. Lett. **B646**, 34 (2007)
17. T. Moroi, L. Randall, Nucl. Phys. **B570**, 455 (2000)
18. ALEPH Collaboration, Phys.Lett. **B533**, 223 (2002)
19. O.P.A.L. Collaboration, Eur. Phys. J. **C29**, 479 (2003)
20. DELPHI Collaboration, Eur. Phys. J. **C34**, 145 (2004)
21. [http://lepsusy.web.cern.ch/lepsusy/www/inoslowdmsummer02/charginolowdm\\_pub.html](http://lepsusy.web.cern.ch/lepsusy/www/inoslowdmsummer02/charginolowdm_pub.html)
22. ATLAS Collaboration, JHEP **1301**, 131 (2013)
23. T. Cohen, M. Lisanti, A. Pierce, T.R. Slatyer, Wino dark matter under siege (2013). [arXiv:1307.4082](https://arxiv.org/abs/1307.4082) [hep-ph]
24. J. Fan, M. Reece, In wino veritas? Indirect searches shed light on neutralino dark matter (2013). [arXiv:1307.4400](https://arxiv.org/abs/1307.4400) [hep-ph]
25. Fermi-LAT Collaboration, Phys. Rev. Lett. **107**, 241302 (2011)
26. H.E.S.S. Collaboration, Phys. Rev. Lett. **110**, 041301 (2013)
27. PAMELA Collaboration, Phys. Rev. Lett. **105**, 121101 (2010)
28. J.F. Navarro, C.S. Frenk, S.D. White, Astrophys. J. **462**, 563 (1996)
29. J. Hisano, K. Ishiwata, N. Nagata, Phys. Lett. **B706**, 208 (2011)
30. J. Hisano, K. Ishiwata, N. Nagata, T. Takesako, JHEP **1107**, 005 (2011)
31. XENON100 Collaboration, Phys. Rev. Lett. **109**, 181301 (2012)
32. L.U.X. Collaboration, Phys. Rev. Lett. **112**, 091303 (2014)

Search for Charginos Nearly Mass-Degenerate with the  
Lightest Neutralino

Based on a Disappearing-Track Signature in pp  
Collisions at  $\sqrt{s} = 8$  TeV

Kazama, S.

2016, XIII, 148 p., Hardcover

ISBN: 978-4-431-55656-5